The environmental impact of air pollution on the built heritage of historic Cairo (Egypt)

*Title Page

The environmental impact of air pollution on the built Heritage of Historic Cairo (Egypt)

Natalia Rovella[a], Nevin Aly[b], Valeria Comite[c]*, Luciana Randazzo [a], Paola Fermo [c], Donatella Barca [a], Monica Alvarez de Buergo [d], Mauro Francesco La Russa [a]

[a] Department of Biology, Ecology and Earth Sciences (DiBEST), University of Calabria, 87036 Arcavacata di Rende, CS, Italy
natalia.rovella@unical.it; luciana.randazzo@unical.it; donatella.barca@unical.it; mlarussa@unical.it

[b] Department of Science and Engineering Mathematics, Faculty of Petroleum and Mining Engineering, Suez University, 43512 Suez, Egypt
Nevin.Aly@suezuniv.edu.eg

[c] Department of Chemistry, University of Milan, Via Golgi 19, 20133 Milan, Italy
valeria.comite@unimi.it; paola.fermo@unimi.it

[d] Geosciences Institute IGEO (CSIC-UCM), Doctor Severo Ochoa 7, 28040 Madrid, Spain
alvarezm@geo.ucm.es

*corresponding author: valeria.comite@unimi.it

*Graphical Abstract

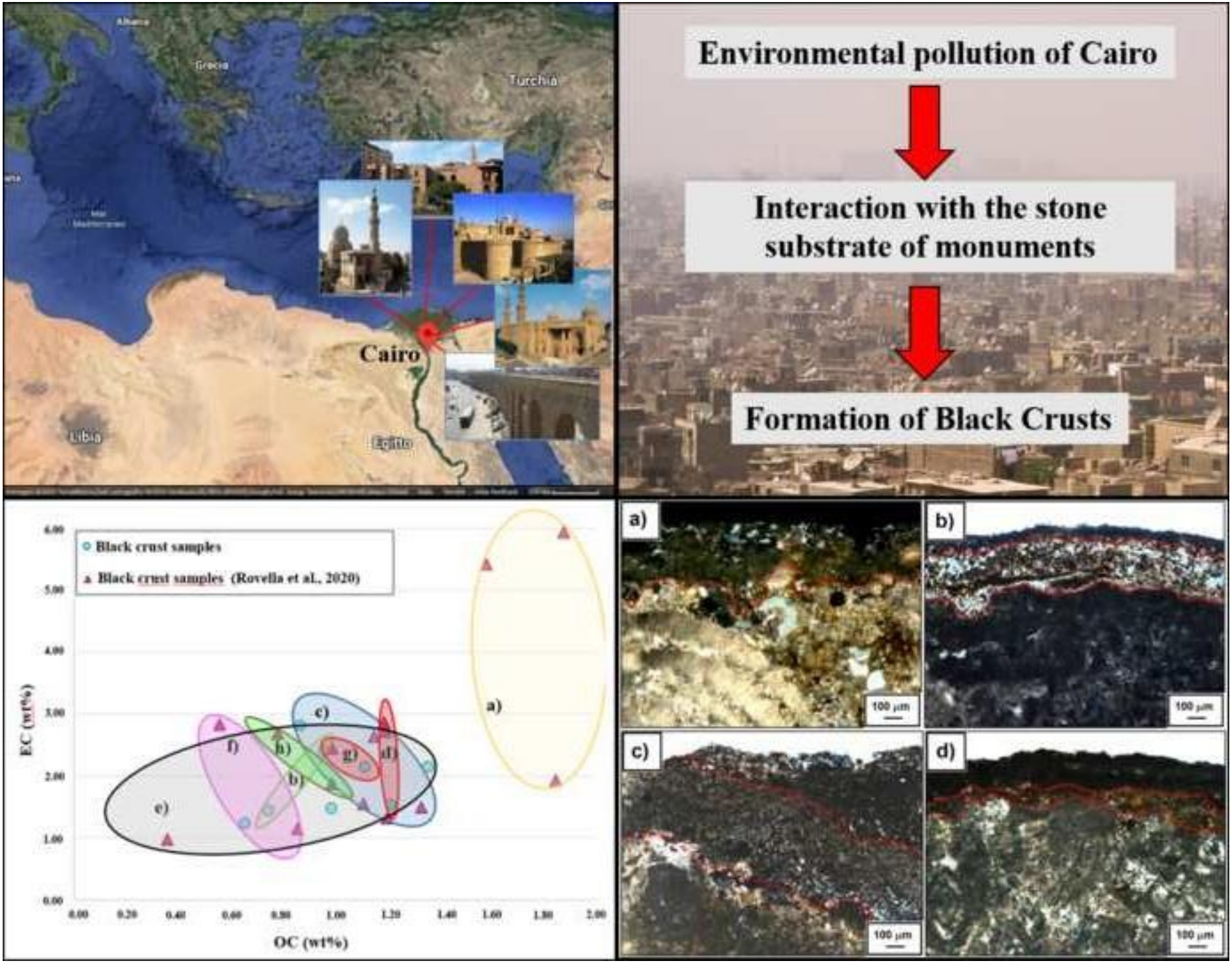

Highlights:

-Black crusts from Cairo have been analyzed by several techniques

-The effect of urban air pollution on the monuments of Cairo have been investigated

- The methodology allowed identification of pollution sources in the black crusts

The environmental impact of air pollution on the built Heritage of Historic Cairo (Egypt)

Natalia Rovella[a], Nevin Aly[b], Valeria Comite[c]*, Luciana Randazzo [a], Paola Fermo [c], Donatella Barca [a], Monica Alvarez de Buergo [d], Mauro Francesco La Russa [a]

[a] Department of Biology, Ecology and Earth Sciences (DiBEST), University of Calabria, 87036 Arcavacata di Rende, CS, Italy

natalia.rovella@unical.it; luciana.randazzo@unical.it; donatella.barca@unical.it; mlarussa@unical.it

[b] Department of Science and Engineering Mathematics, Faculty of Petroleum and Mining Engineering, Suez University, 43512 Suez, Egypt

Nevin.Aly@suezuniv.edu.eg

[c] Department of Chemistry, University of Milan, Via Golgi 19, 20133 Milan, Italy

valeria.comite@unimi.it; paola.fermo@unimi.it

[d] Geosciences Institute IGEO (CSIC-UCM), Doctor Severo Ochoa 7, 28040 Madrid, Spain

alvarezm@geo.ucm.es

*corresponding author: valeria.comite@unimi.it

Abstract

In the last decades, many researchers investigated the relation between environmental pollution and the degradation phenomena on the built heritage, because of their rapid increase and growing harmfulness. Consequently, the identification of the main pollution sources has become essential to define mitigation actions against degradation and alteration phenomena of the stone materials. In this way, the present paper is focused on the study of the effect of air pollution on archaeological buildings in Historic Cairo.

A multi-methodological approach was used to obtain information about the chemical composition of examined black crusts and to clarify their correlation with the air pollution, specifically the heavy metals and the carbonaceous fraction, their main sources, and their impact on the state of conservation of the studied sites.

All specimens were characterized by polarized optical microscopy (POM), X-Ray Diffraction (XRD), Electron Probe Micro Analyser coupled with energy dispersive X-ray spectrometry (EPMA-EDS), laser ablation inductively coupled plasma mass spectrometry (LA-ICP-MS) and Thermo-gravimetric analysis (TGA).

The results indicate a good correlation between the composition of black crusts and the main pollutant sources in Cairo such as vehicular traffic and industrial activities.

Keyword: air pollution; built cultural heritage; black crust; heavy metals; carbonaceous fraction; degradation.

1. Introduction

Cairo is the largest city in Egypt and in Africa; here, the air pollution produced many environmental problems related to aerosol particulate matter and to the high levels mostly of sulphur dioxide and lead. For this reason, it was listed as one of the most polluted cities in the world (Gurjar et al., 2010). The air pollution sources in the city are different and include burning of rubbish, vehicle emissions (~4.5 million cars on the streets of Cairo) and urban industrial activities. The city has 15–20 million inhabitants and is characterized by high congestion due to a population density of 13107/km^2 (Abbass et al., 2020). Furthermore, the lack of rain helps the accumulation of pollutants. The entire area of Cairo is severely affected by industrial and urban emissions of metals and metalloids (Abdel-Latif and Saleh, 2012). For example, only the cement industry releases around 2.4 million tons per year of cement bypass dust into the atmosphere (Alkhdhairi et al., 2018).

Moreover, it was estimated that the high Particulate Matter (PM) concentrations cause around 10 % of premature deaths in Egypt, where the national cost of air pollution is estimated at $20.9 million (Abbass et al., 2020).

An important factor that contributes to the air pollution increase is represented by the climatic conditions (Lowenthal et al., 2014; Alkhdhairi et al., 2018) and the remarkable seasonal temperature changes; in fact, its climate is classified as hot arid (BWh, according to the Köppen and Geiger (1936) climate classification).

At the same time, Cairo city produces 10,000 Tm of waste daily, often burned illegally. Previous studies on air pollution and atmospheric aerosols emissions from industrial and urban sites in Greater Cairo Area (GCA) highlighted how heavy metals represent a relevant and worrying component (Robaa, 2003; Abu-Allaban et al., 2007, 2009; Zakey et al., 2008; Abdel-Latif and Saleh, 2012; Shaltout 2013a,b, 2014).

Borai and Soliman (2001) demonstrate a direct relationship in Cairo city between the trace metals (e.g. Pb, Cd, Zn, Ni, Mn, Pb, Zn, and Cu) present in the aerosol PM and the anthropogenic activities such as vehicular traffic and industries, specifically, ferrous metallurgical work, foundries, lead smelters, lead batteries, ceramics, glass, bricks, textiles and plastics.

In this regard, many lead and copper smelters that heavily pollute the city air are unregistered. This fact produced a permanent haze over the city with PM reaching over three times the normal levels (Creighton et al., 1990).

In some studies (Khairy et al., 2011; Abdel-Latif and Saleh, 2012), the role of the road dust is clarified: dust deposits and accumulates on ground surfaces, along roadsides that are contaminated by heavy metals and organic matter. It does not remain deposited in place for long but is easily re-suspended back into the atmosphere, where it provides a significant amount of trace elements. The mentioned reference indicates that road dust within Cairo contains higher concentrations of elements (Pb, Zn, Cd, As, Sn and V) mainly reflecting the contribution of vehicular traffic and industrial activities.

Pollutants are deposited on the surface of stone materials constituent of the historical buildings. Indeed, those ones suffer serious deterioration phenomena in Cairo as a result of physical-chemical and biological effects (El-Tawab et al., 2012), favouring black crust formation, alveolization, chemical alterations, disaggregation pitting, cracks, erosion (Davidson et al., 2000).

Black crusts are one of the most dangerous degradation products in building stones and are closely connected with environmental pollution, especially the atmospheric one. They are very common on the carbonate substrates such limestones. This lithotype is widely used for the construction of historical monuments in the whole Mediterranean area thanks to its workability, durability and aesthetic features; nevertheless it is frequently affected by degradation phenomena (Fitzner et al., 2002; La Russa et al., 2013a; Ricca et al., 2019) firstly black crusts.

They are formed through sulphating processes of the stone surface where calcium carbonate ($CaCO_3$), which is the main constituent of limestone, is transformed into gypsum $CaSO_4*2H_2O$

(Whalley et al., 1992; Comite et al., 2012, 2019, 2020a,b; Rovella et al., 2020). Metals and metal oxides, present in the atmosphere, catalyse the sulphating reaction (Fermo et al., 2020). This process affects mainly stone materials having carbonate nature (for example limestone, marble, lime mortar). In addition, during the crust formation, particulate matter, which contains mainly amorphous carbon and several heavy metals, can be embedded into the gypsum, providing its characteristic black colour (La Russa et al., 2018) and altering the aesthetic appearance of the monuments. For instance, the old structures in Cairo, originally of a whitish colour and some even striped with the "ablaq" style (in some instances it is hard to spot the stripes due to the amount of dust covering the surface) are now completely blackened (Orphy and Hamid, 2004). Moreover, black crusts threaten the conservation of the stone surfaces: hard crusts, usually firmly attached to the stone are very hard to remove and can weaken the surface on which they develop.

For all these reasons the attention of the scientific world is steadily increasing on the effect of air pollution on archaeological buildings in Cairo and, consequently on the relative degradation products, (Fitzner et al., 2002; Khallaf, 2011; Kukela and Seglins, 2011; Abdelmegeed et al., 2019). The present research was conceived in this context and deals with the relation between air pollution and the historical building in Cairo.

The study areas are located in the historic Cairo (Fig. 1S available in *Supplementary material*) and includes the outer walls of Salah El-Din citadel, the Magra El-Oyoun wall, and monuments of the Northern Mamluk cemetery such as the Mosque of the Sultan Faraj ibn Barquq, the Qaitbay Mosque and the tomb of Qansuh Al-Ghuri. They were selected for historical-artistic relevance, location in the urban context characterized by different prevailing pollution sources and building stone materials (i.e., limestone).A complementary analytical approach was applied to gain information on the chemical composition of the collected black crusts and define a correlation between the air pollution, especially the heavy metals contribution and the carbonaceous fraction, and their main sources , as well as to study the conservation state of the investigated sites.

The samples were characterized by polarized optical microscopy (POM), X-Ray Diffraction (XRD), Electron Probe Micro Analyser coupled with energy dispersive X-ray spectrometry (EPMA-EDS), laser ablation inductively coupled plasma mass spectrometry (LA-ICP-MS) and Thermo-gravimetric analysis (TGA).

2. Materials and Methods

The limestones used for the construction of the historical stone monuments in Cairo come from local middle and late Eocene outcrops (47.8- 33.9 million years ago) located in Mokattam, Helwan and Giza areas (El-Nahhas et al., 1990; Ahmed et al., 2006; Park and Shin, 2009; Aly et al., 2015, 2020). These materials are still being used for stone replacement or rebuilding works in monuments preservation practice as well as for modern buildings.

All the monuments underwent various rebuilding interventions over time and there is not very reliable information about them. Regarding restoration in modern epoch, it is known that several interventions were carried out in the 19^{th} century, 1990s and early 2000s.

Samples consist of black crust and stone substrate, were taken from some portions located on vertical surfaces of the selected monuments, seriously affected by degradation phenomena and exposed to high rates of environmental pollution (Table 1).

A complete characterization of stone substrate and black crust associated was carried out, applying different analytical techniques aimed to determining the stationary and mobile combustion sources, major responsible for the blackening and soiling encountered.

POM analyses were performed on polished thin sections by using a Zeiss Axiolab associated with AxioCam MR for digital image acquisition. This technique is aimed to characterize both substrate and black crusts and to investigate the substrate/black crust interface determining minero-petrographic features and evaluating the degradation degree of each sample.

XRD analysis was carried out to identify the mineralogical phases constituting the black crusts sampled. Measurements were performed using a Siemens D5000 diffractometer and spectra were taken in the range 5°–65° 2Θ, using a step-size of 0.02° 2Θ and a step-time of 2 s/step.

Samples were carefully prepared by separating the limestone substrate from the black crust and pulverized them in an agate mortar.

An EPMA - JEOL - JXA 8230 —coupled with an EDS spectrometer - JEOL EX-94310FaL1Q - Silicon drift type— was used in order to observe the micro-morphology and analyse the composition in terms of major chemical elements. The EDS analyses were carried out according to the following operating conditions: 15 keV HV; 10 nA probe current; 11mm working distance; 40° take off; and 30 seconds live time. Before measuring, samples were graphite (ultra-pure graphite) sputtered to facilitate the electron conductivity by generating a ± 5 nm thick film, applied by Sputter - Carbon Coater QUORUM Q150T-ES, 70 A pulse current and 2.5 sec pulse time).

Chemical analyses of the black crusts, as well as of the substrates, in terms of trace elements were performed by LA-ICP-MS. This method can analyse a great number of chemical elements with a spot resolution of approximately 40–50 μm, which also allows the determination of compositional variations at a micrometric scale. Analyses were carried out using an Elan DRCe instrument (Perkin Elmer/SCIEX), connected to a New Wave UP213 solid-state Nd-YAG laser probe (λ=213 nm). Samples were ablated by a laser beam in a cell following the method tested by Gunther and Heinrich (1999). The ablation was performed with spots of 40–50 μm with a constant laser repetition rate of 10 Hz and a fluency of ~ 20 J/cm^2 (Barca et al., 2011). Calibration was performed using the NIST 612-50 ppm glass reference material as external standard (Pearce et al., 1997). Internal standardization to correct instrumental instability and drift was achieved using CaO concentrations from EPMA-EDS analyses. Accuracy was evaluated on BCR 2G glass reference material and on an in-house pressed-powder cylinder of the standard Argillaceous Limestone SRM1d of NIST (Barca et al., 2011). The resulting element concentrations were compared with reference values from the literature (Gao et al., 2002). Accuracy, as the relative difference from

reference values, was always better than 12 %, and most elements plotted in the range of ±8 %. Analyses were performed on 100 μm thick cross-sections including both the black crust and the unaltered substrate samples in order to reveal the geochemical variability. TGA was carried out for the quantification of the carbonaceous fraction (TC total carbon= OC organic carbon + EC elemental carbon), Ox oxalate, CC carbonatic carbon and gypsum, present in the black crusts. It was performed by a Mettler Toledo TGA/DSC 3+, which allows simultaneous TG and DSC (Differential Scanning Calorimetry) analyses. The analyses were conducted in the range 30°- 800° C, increasing temperature with a rate of 20° C/minute. The carbonaceous components were estimated in temperature ranges defined by previously studied standards and using two different atmospheres, i.e. the inert and the oxidant one. The complete methodology is described also in previous works La Russa et al. (2017).

3. Results and discussion

3.1.POM Analysis

Sample 2, coming from Salah El-Din citadel, is classified as biomicrite (Folk, 1959) and wackestone (Dunham, 1962). Moreover, quartz, iron oxides and macroforaminifera, i.e. nummulites (Khallaf, 2011) were also identified.

The crust overlapping the substrate is brownish in colour, has a roughly uniform thickness of about 175 μm, it is composed by microcrystalline gypsum, brownish iron oxides and carbonaceous particles (Fig.1a).

The crust-substrate contact is rather clear with a marked separation between them.

The substrate in sample 3 is classified as biomicrite (Folk, 1959) or mudstone (Dunham, 1962). It includes allochems as quartz, rare iron oxides and fossils. The crust is located in small areas of the substrate and has a slightly variable thickness of about 20-30 μm, containing iron oxides inside. It is well adhered to the substrate and appears with irregular and strongly discontinuous edges.

202 The substrates of samples 12 and 14 are classifiable as biomicrite (Folk, 1959) and mudstone
203 (Dunham, 1962).
204 In particular, the substrate of sample 12 includes rare quartz and plagioclase crystals. The black
205 crust overlying the substrate is rather compact with an overall thickness varying between 50 and
206 200 μm. It shows a not so clear stratification but at least two layers are recognizable. The crust is
207 well adhered to the substrate, has irregular morphology, is made up of microcrystalline gypsum and
208 incorporates numerous spherical and sub-spherical carbonaceous particles.
209 In sample 14, the crust has an average thickness of 400 μm and shows an evident stratification
210 (Fig.1b): an external dark brown layer with an average thickness of 50 μm and a rather regular
211 external profile; an innermost layer, light brown in colour, reaching in some places a thickness of
212 300 μm and deepening into the substrate for about 100 μm. The contact crust/substrate is mainly
213 sharp.
214 The crust is made up of microcrystalline gypsum and includes from sub-spherical to spherical
215 carbonaceous particles, particularly numerous, especially in the inner layer (Fig.1b) and averagely
216 30 μm in size.
217 Sample 15 is classified as biomicrite (Folk, 1959) and mudstone (Dunham, 1962). The crust is thick
218 from 400 to 1000 μm, and not well adhered to the substrate. It consists of microcrystalline gypsum
219 and is layered in three levels (Fig. 1c): the outermost one shows a dark brown colour and an average
220 thickness of 200 μm; the intermediate and the inner layers show a gradually lighter grey-brown
221 colour and vary in thickness from 200 to 500 μm. Carbonaceous particles are present throughout the
222 thickness of the crust, but are noticeably abundant in the inner layer. They show a spherical-
223 subspherical shape and a variable size from 20 to 50 μm
224 The substrate of samples B and E is biomicrite (Folk, 1959) and wackestone (Dunham, 1962) with
225 bioclasts of considerable size exceeding 1mm (Fig.1d). The crust overlies regularly the limestone to
226 which is well adhered; however, the morphology and thickness are rather irregular, the last one
227 varying from 50 to 400 μm.

The crust in sample B is constituted by microcrystalline gypsum and contains rare carbonaceous particles and iron oxides. It is possible to identify a darker brown outer layer, with a regular and thin thickness of about 20 μm, and a brownish inner layer that has a greater and irregular thickness, from 50 to 300 μm in the points where it deepens into the substrate.

The crust in sample E is discontinuous, with a variable thickness from 50 to 500 μm, consists of microcrystalline gypsum and, at least, two irregular levels are distinguished (Fig.1d): the outer one is browner and contains numerous carbonaceous particles; the internal layer, where present, is lighter and reddish, about 100 μm thick and the carbonaceous particles are less common. The substrate of sample H is classified as biomicrite (Folk, 1959) and mudstone (Dunham, 1962). The allochem fraction includes quartz and macroforaminifera fragments.

Overall, the crust is fractured, jagged with very irregular edges (Fig. 1e). It also appears divided into two layers: the outermost dark coloured with a thickness of about 500 μm, the innermost light grey with a thickness of 200 μm. Microcrystalline gypsum, iron oxides and numerous carbonaceous particles are visible in both.

242242

3.2 XRD Analysis

The analysis (Table 1S available in Supplementary material) revealed the presence of gypsum, calcite and secondarily quartz as the main mineralogical species in almost all the crusts examined. Quartz and calcite come from the limestone substrate, while gypsum is the main constituent of the crusts (Barca et al., 2011; Belfiore et al., 2013; La Russa et al., 2013b; Ruffolo et al., 2015). Among the other mineralogical phases, plagioclase, K-feldspar, hematite and clay minerals were identified in subordinate amount.

The crusts include halite, the most common sodium chloride salt in the subsurface water of Egypt and in sea spray coming from the Mediterranean Sea (Aly et al., 2015) and consequently also in Egyptian limestones (Gauri and Holdren, 1981; Gauri et al., 1986; Helmi, 1990). The salt is linked

253 to the capillary rise of water from the subsoil and the consequent precipitation of the salt inside the
254 stone (Charola, 2000; Fitzner et al., 2002; Gomez-Heras and Fort, 2007).
255255

256 3.3 EPMA-EDS Analysis

257 EPMA-EDS morphological and microchemical analyses were carried out on the black crusts of the
258 five sites.
259 In the samples 2 and 3 the crusts show an irregular morphology. Compositional analysis revealed
260 CaO as major component, followed by SO_3, SiO_2, Al_2O_3, ClO e FeO, Na_2O, MgO, K_2O.
261 Black crusts of samples 12-14 are adherent to the substrate, especially sample 12 (Fig. 2S a); they
262 appear rather compact. Gypsum microcrystals and carbonaceous sub-spherical particles were
263 identified.
264 The crusts are constituted mainly by CaO and SO_3 thanks to gypsum-based composition, secondly
265 by SiO_2, and lastly ClO, Al_2O_3, Na_2O, MgO, K_2O, FeO. In sample 12, gypsum was detected also in
266 substrate, where the crust is thicker and deepens in.
267 The black crust in sample 15 shows a homogeneous morphology (Fig. 2S b). It does not properly
268 adhere to the underlying substrate, due to the presence of numerous fractures, that in some points
269 cross the entire body of the crust.
270 The most abundant component is mostly CaO, followed by SiO_2, SO_3, ClO, and lastly Al_2O_3, FeO,
271 K_2O, MgO, Na_2O, TiO_2 and P_2O_5.
272 The crusts taken from Qaitbay Mosque show slight different morphological features.
273 Sample E is rather compact, with a regular external profile and a sharp contact with the substrate
274 (Fig. 2S c). The crust in sample B is more porous with a dendritic morphology. It is adherent to the
275 substrate except in some points, where the two portions are separated by fractures. In both crusts,
276 acicular crystal of gypsum and sub-spherical carbonaceous particles were recognized.
277 The chemical analysis suggested how CaO is the predominant component, followed by SiO_2, SO_3,
278 secondly by, ClO, Al_2O_3, Na_2O, K_2O, FeO and lastly by MgO, P_2O_5 and TiO_2.

The sample H shows in general an irregular morphology, fractures, and jagged edges. However, it was individuated little portions more homogeneous, compact and adherent to substrate, that were analysed by EDS and then by LA-ICP-MS. Gypsum microcrystals and carbonaceous particles were identified in the crust. The chemical composition is characterized by a high amount of CaO, Al_2O_3, SiO_2 and SO_3, followed by Na_2O, P_2O_5, K_2O, and TiO2.

284284

285285

3.4 LA-ICP-MS Analysis

287287

Trace elements concentrations were determined by LA-ICP-MS on the black crusts and underlying substrates of all the examined samples. The results obtained for each spot analysis are listed in Table 2S, where average values and corresponding standard deviations are displayed.

Looking at the concentrations of the most significant trace elements (Table 2S), elements like lead (Pb), barium (Ba), vanadium (V), chromium (Cr), cobalt (Co), zinc (Zn) and arsenic (As) have relatively high concentrations, indicating an accumulation of atmospheric pollutants on the gypsum crusts, regardless of the sampling location. The documented high concentrations of lead suggest that this element is still present in the urban environment of Cairo city many years after the ban of leaded gasoline in Egypt (Fujiwara et al., 2011), as it has been also shown by previous studies in other cities around the world (Sanjurjo Sánchez et al., 2011; Török et al., 2011; Graue et al., 2013).

As well known, all these elements can be introduced in the urban environment by a wide range of different anthropogenic processes, mainly mining, smelting, industrial manufacturing, metal processing, etc. (Johnson et al., 2011) but also by domestic and residential activities (heating, vehicles, transport). However, some elements occur naturally in the same urban environment as a result for example of geologic processes (erosion of outcropping bedrocks). The proportion of natural and anthropogenic components may vary widely depending thus on the geology and the industrial history of the urban centre. Our geochemical approach was addressed to define the

relation between pollution sources and degradation state of stone materials; for this purpose, Enrichment Factor was calculated both for heavy metals, metalloids and Rare Earths Elements (hereafter REE). Enrichment factors calculation is a procedure commonly used in geochemical studies for the determination of the anthropogenic origin of chemical elements. For the purpose of our study, the chemical procedure was followed by normalizing the chemical composition of trace elements in black crusts with respect to those of calcareous substrates on which they grew (Table 3S).

The normalization procedure performed here used Scandium (Sc) as 'conservative' element, as it was presumed to have no anthropogenic enrichment or a minor anthropogenic input (Loring, 1991; Gallego et al., 2013). This calculation is carried out by comparing the concentrations of the trace elements with those of the conservative element by following the formula EF = $(M/N)_{sample}/(M/N)_{substrate}$, which is the ratio between the concentrations of the metal (M) and those of the normalizer (N), both for the sample and for substrate samples (Reimann and Caritat, 2000). Figure 2 show EFs for all the examined samples grouped for sampling location criterion. As shown in the Figure 2, samples 2 and 3 are enriched in Zn, As, Pb, REE (L-REE, light and H-REE, heavy) and Sn, Ba, Pb and HREE, respectively. Similarly, samples 12 and 14 show enrichment in all the LREE and in most metals and metalloids elements. The same enrichment trend (Fig. 2) is highlighted by the remaining samples (B, E, 15 and H).

Samples B and E reveal enrichments in Co, Mo, Sn, Sb, Ba, Pb, and Sn, Ba, Pb, respectively with associated null or slight enrichment in REE. As regards sample 15, metals and metalloids are similarly enriched as in the previous samples, while the REE show values close to the background. Conversely, sample H shows only a slight enrichment in Sn, Sb and Ba, with no enrichment in REE.

Finally, some heavy metal and metalloids concentrations (V, Cr, Co, Ni, Zn, As, Cd and Pb, Mn and Cu) in the studied black crusts were compared to the corresponding concentrations in road dust samples (after Abdel-Latif and Saleh, 2012), collected across the Cairo city (Fig. 3).

331 It is worth to note that Zn, Mn and Cu are, together with Fe (not determined in this study), the
332 metals present in the higher concentrations in PM (Atzei et al., 2014). Road dust includes deposits
333 and accumulates on ground surfaces, along roadsides, which is contaminated by heavy metals. It
334 usually does not remain deposited in place for long, but it is easily re-suspended back into the
335 atmosphere, as it was already mentioned. For the purposes of this work, the concentrations of the
336 above-mentioned metals in the <125 μm fraction were considered for the comparison as these sizes
337 are easily resuspended in atmosphere contributing with a significant amount of trace elements in
338 residential, main traffic roads and industrial areas. Metals concentrations in the dust were higher in
339 main traffic roads and industrial areas compared to those of residential areas. Figure 3 shows the
340 box plot diagram, in which minimum, maximum and average values for the selected elements in
341 black crusts samples are reported together with the values corresponding to the metal concentration
342 in the dust collected in Cairo (Abdel-Latif and Saleh, 2012). As can be seen, most of the heavy
343 metal average values in the black crusts fall within the ranges relevant to the dust of the Cairo city.
344 Exceptions in this trend are the value of arsenic (As) and, at lesser extent, the value of cadmium
345 (Cd). In fact, black crusts samples experienced values of these two elements greater than those of
346 dust samples. Both these metals have been widely used in industrial sector, i.e. man-made
347 emissions from metal smelters (iron, steel, copper, lead and zinc production), mining activities,
348 combustion processes (coal and oil) and refuse incineration (stabilizers and pigments in plastics).
349 Studied black crusts may have accumulated these elements over time being considered as good
350 traps for atmospheric particles, useful for the identification of the particulate matter pollution
351 emission sources in urban areas.

352352

353 3.5 Carbonaceous fraction

354 Carbonaceous particles emitted by combustion processes are among the main constituents of
355 aerosol particulate matter (PM) (Bove et al., 2016; Bozzetti et al., 2017) and one of the main factors
356 responsible for the blackening of buildings.

357 The quantification of the carbonaceous species that form the non-carbonatic fraction, i.e. OC
358 (organic carbon) and EC (elemental carbon) in damage layers, are required particularly in urban
359 areas in order to investigate atmospheric deposition processes on building surfaces, to get
360 information on the possible particulate matter sources and to suggest mitigation measurements to
361 fulfil a better conservation of the stone surfaces (Fermo et al., 2015).
362 Black carbon (also known as elemental carbon, EC, because of its structure quite similar to that of
363 graphite) is emitted by combustion processes, such as traffic and biomass burning (Piazzalunga et
364 al., 2010, 2011; Belis et al., 2011), and is the main responsible for soiling on monuments surfaces
365 (Ghedini et al., 2000; Tidblad et al., 2012). On the other hand, OC that includes hundreds of organic
366 substances of different nature, is emitted by combustion processes as a primary pollutant but is also
367 of secondary origin and can form starting form gaseous organic precursors (i.e. volatile organic
368 compounds, VOC) (Fuzzi et al., 2006; Robinson et al., 2007; Bernardoni et al., 2011; Gentner et al.,
369 2012; Vassura et al., 2014; Daellenbach et al., 2016). It is also known that the Mediterranean region
370 is characterized by an intense photochemistry during summer which brings to high concentration in
371 the aerosol PM of secondary organic substances (Bozzetti et al., 2017) and this phenomenon in
372 Cairo is particularly favoured.
373 Table 2 shows the values obtained by thermogravimetric analysis and reported as percentages by
374 weight (wt.%) of TC (Total Carbon), OC (Organic Carbon); EC (Elemental Carbon); OX (Oxalate),
375 Gy (Gypsum); OC/EC and EC/TC ratios are reported as well; TC=OC +EC.
376 At first sight, by comparing the samples taken from the same monument it is possible to highlight
377 slight differences between them.
378 It should be noted that the greatest variability in the various samples was found for gypsum
379 (minimum value of 9.7%, maximum value 51.25). In particular, the highest concentrations were
380 obtained for samples 12, 14 and B in accordance with what was observed by XRD analysis.
381 In general, all the crust samples show higher EC values (wt. %) than OC (Table 2). The EC values
382 are higher than what was generally observed for the samples of atmospheric particulate matter in

383 Cairo (Favez et al., 2008; Kanakidou et al., 2011; Lowenthal et al., 2014; Cheng et al., 2016). It is
384 also important to stress out that the carbonaceous substances dominate the PM2.5 composition of
385 megacities atmosphere, especially in Cairo (Cheng et al., 2016).
386 Furthermore, data in the literature show that PM in the city of Cairo has an average annual OC/EC
387 ratio of 2.45 (Lowenthal et al., 2014). This ratio is rather linked to seasonal conditions, with values
388 of 3.45 (autumn season), 2.64 (winter season) and 2.17 for the summer season (Abu-Allaban et al.,
389 2007). The highest levels observed during autumn season have been related to episodes of biomass
390 combustion on the Nile delta. In fact, during this period of the year the residual straw from rice
391 cultivation is commonly burned after the harvests. Carbonaceous particles emitted by this
392 combustion could therefore partially reach the city thanks to the influence of prevailing winds from
393 the North (Favez et al., 2008).
394 According to Kanakidou et al. (2011) the polluting sources contributing to the OC fraction into the
395 air in Cairo are mainly represented by industry, residential, energy production and incinerators,
396 while
397 EC is mainly emitted from mobile sources (diesel traffic) and combustion processes (e.g. domestic
398 heating or industrial activities) (Abu-Allaban et al., 2007; Favez et al., 2008).
399 The obtained OC and EC values of the crust samples were compared with other black crust samples
400 from Cairo taken, in some cases, from the same monuments (Rovella et al., 2020), whose study was
401 focused on the state of conservation of the building materials. These data were obtained with the
402 same TGA methodology and their use was essential to better understand the interaction between the
403 polluted environment of Cairo city and the black crusts.
404 Figure 4 shows that, in general, as the sampling height of the crusts decreases, the concentration of
405 EC increases. This confirms that the main source of this pollutant could be vehicle traffic which is
406 responsible for the emission of particles which mainly affects surfaces at lower heights in direct
407 contact with the road. The OC value on all the analysed samples varies from a minimum of 0.36 to
408 a maximum of 1.88, while that of EC varies from a minimum of 0.99 to a maximum of 5.95. From

409 the trends shown in the Figure 4, it is also observed that the OC values are more constant than the
410 EC values.
411 The clustering based on the relationship between the concentrations of EC and OC and showed in
412 Figure 5a, suggest similar trends for most of the samples nevertheless they come from different
413 areas of Cairo. The only exception is represented by site a) (Fig. 5b) where high EC values are
414 observed especially for the relative three samples (samples 8, 9 and 10 of figure 5a which were both
415 taken at low heights).
416 In order to evaluate potential differences on the accumulation of OC and EC within the crusts
417 analysed in the city of Cairo and other polluted cities, comparisons were made with crusts taken
418 from Italian monuments (Fig. 6) such as: Trevi Fountain in Rome (La Russa et al., 2017); several
419 private buildings in Venice (La Russa et al., 2018), Church of Santa Maria delle Grazie in Milan
420 (Comite and Fermo et al., 2018) and the Monza Cathedral located in the homonymous city (Comite
421 et al., 2020c).
422 The comparison (Fig. 6a) allowed highlighting the presence of two types of samples for which quite
423 good correlations between OC and EC were observed. Characteristic OC/EC ratios have been
424 identified for the two groups corresponding to the angular coefficients of the trend lines: the first
425 group has an OC/EC ratio = 0.47, while the second shows an OC/EC ratio = 0.42. This allows
426 hypothesizing that for the second group, in which all the Cairo samples fall, the primary sources
427 prevail while for the samples belonging to the first group, and a mixed contribution of the sources
428 (primary + secondary) can be suggested. The high EC contents in the Cairo samples can be
429 explained by a combination of various polluting sources such as mobile emissions or combustion
430 processes (e.g. domestic heating or industrial activities) (Abu-Allaban et al., 2007; Favez et al.,
431 2008).
432 In fact, the city is characterized by high congestion due to, as mention before, a population density
433 of 13107/km^2 and 2.4 million cars (El-Mansy et al., 2013; CAPMAS, 2017; Moustafa et al., 2018).
434 Urban growth rates are higher than the development rate of public transport services with a

435 consequent increase in the use of private vehicles and taxis (Duquennois and Newman, 2009; El-
436 Dorghamy et al., 2015) which release a lot of black carbon into the air thus dominating the other
437 potential polluting sources (Mahmoud at al., 2008). Vehicle traffic in the past has also been
438 characterized by the presence of vehicles with old generation technical characteristics that have
439 increased the pollution of the city (El Mowafi and Atalla, 2005; Kanakidou et al., 2011). Even in
440 the past, domestic heating or industrial sector introduced significant quantities of black carbon into
441 the air (Abu-Allaban et al., 2007; Favez et al., 2008). For these reasons, the first actions for
442 environmental protection were introduced in the early 1990s and after that, a slight air quality
443 improvement emerged (Kanakidou et al., 2011).
444 A further confirmation of our statement arises, comparing the OC/EC ratio (Fig. 6b) with that
445 performed on the carbonaceous aerosols (Schauer et al., 1999, 2002; Saarikoski et al., 2008).
446 Generally, relatively low values equal to or less than 1 are attributable to primary emissions and
447 combustion of fossil fuels (Perrino et al., 2008), while ratios greater than 1 usually indicate different
448 polluting emissions. Observing (see Table 2) the ratios (minimum value of 0.23 and maximum
449 0.75) obtained for these samples, the polluting sources that have likely affected the accumulation of
450 the carbonaceous fraction in the black crusts of Cairo are primary sources including vehicular road
451 traffic.
452 In fact, it has been highlighted that for urban sites in Europe (Pio et al., 2011), where vehicular
453 emissions are the dominant source of pollution, the values obtained from the OC/EC ratios fall in
454 the range 0.3-0.7, suggesting a low contribution of secondary OC.
455 Finally, the correlation between the gypsum content, the carbonaceous fraction and the
456 concentrations of heavy metals can provide further information on the sources of pollutants. Figure
457 3S shows the correlation matrix between all the experimental variables quantified on the examined
458 samples in the present paper. The observation of the matrix shows how gypsum is positively related
459 to different heavy metals, namely Cu, Pb, Sb and Zn, and to, a lesser extent, the remaining metals
460 and metalloids. This could indicate that probably some elements are closely related to the

sulphation processes. In fact, heavy metals have long been considered capable of catalysing the sulphation processes (Rodriguez-Navarro and Sebastian, 1996; Cultrone et al., 2004; Simaõ et al., 2006; Wahba and Zaghloul, 2007). A good correlation has been observed between Gy and Cu (0.92). According to Boke et al. (1999), the Cu^{+2} ion increases the absorption of SO_2 in the aqueous film present on a carbonate surface. This ion has also been shown to dissipate any gradient of electrical potential allowing hydrogen ions to spread much faster on surfaces (Chang et al., 1981). As a result, an increase in SO_2 uptake is observed which accelerates the sulphation process. Furthermore, Cu has been shown to be released from the exchangeable carbonate phase making this metal potentially available to catalyse surface reactions (McAlister et al., 2008).

The correlation matrix also allows highlighting the correlation existing between metals. For example, there is a very good correlation between Ni and V indicating the contribution of heavy oil combustions (Bove et al., 2016).

On the contrary, the carbonaceous fraction EC is negatively correlated with gypsum and also with various heavy metals. In fact, the surface of EC particles contains numerous adsorption sites that are capable of enhancing catalytic processes because of their high surface reactivity. As result of its catalytic properties, EC may affect some important chemical reactions involving atmospheric sulphur dioxide (SO_2), nitrogen oxides (NO_x), ozone (O_3) and other gaseous compounds (Gundel et al., 1989) other than could have a catalytic effect on the oxidation of sulphite to sulphate (Böke et al., 1999).

As observed in the figure 3, where the greatest polluting contribution seem to be linked to vehicle traffic along the major road arteries, it is clear that the pollution produced by vehicles could also be the main source of enrichment of black crusts.

4. Conclusion

The results achieved in this work highlighted the strong correlation between the atmosphere composition and the degradation processes affecting stone materials used in the built cultural heritage of Cairo city. The multi-analytical approach demonstrated how black crusts can be considered such as an efficient "natural sample holder" of atmospheric pollutants, capable to provide information about atmospheric composition especially in terms of heavy metals. Precisely, the study revealed that the black crusts analysed are constituted mainly by heavy minerals ascribable to the road dust of Cairo city, with the exception of As and Cd, being widely used in the industrial sector.

The data on the carbonaceous fraction suggested that the formation of black crusts sampled is influenced by a preeminent action of the primary sources. At the same time, the high EC contents confirmed the contribution of various polluting sources, such as mobile emissions or combustion processes (e.g. domestic heating or industrial activities) in the formation of the black crusts. Additionally, EC data affirm the clear predominance of pollution produced by vehicles, becoming the main source of enrichment of the black crusts.

In particular, the sulphation processes in the Cairo city is improved by heavy metals, i.e. Cu, Pb, Sb and Zn that play a catalysing role.

This research demonstrated how the contribution of atmospheric pollution is crucial in the evolution of the degradation phenomena, affecting the built cultural heritage in Historic Cairo. Consequently, the reduction of emissions into the atmosphere, adopting for example more eco-sustainable policies, becomes extremely necessary not only for the conservation of cultural heritage but more in general, for the safeguard of the environment and human health.

Acknowledgements

The present research is a part of an Executive program for scientific cooperation between the Italian Republic and the Arab Republic of Egypt, entitled “Characterization of black crusts formed on historical buildings under different levels of ambient air pollution in Cairo and Venice”.

Moreover, it is also part of an international cooperation program funded by CSIC, I-COOP (“Implementation of a reference laboratory for the diagnosis, conservation and restoration of stone-cultural heritage in Egypt”, January 2019 December 2020, Ref. COOPB20379).

Finally, the research was partially funded by the project TOP Heritage (P2018/NMT-4372) of the Community of Madrid. The authors wish to acknowledge professional support of the Interdisciplinary Thematic Platform from CSIC Open Heritage: Research and Society (PTI-PAS).

References

Abbass, R.A., Kumar, P.T., El-Gendy, A., 2020. Car users exposure to particulate matter and gaseous air pollutants in megacity Cairo. Sustain. Cities Soc. 56 (102090), 1-13. https://doi.org/10.1016/j.scs.2020.102090.

Abdel-Latif, N.M., Saleh, I.A., 2012. Heavy Metals Contamination in Roadside Dust along Major Roads and Correlation with Urbanization Activities in Cairo, Egypt. J. Am. Sci. 8(6), 379-389. ISSN: 1545-1003.

Abdelmegeed, M., Hassan, S., 2019. Diagnostic investigation of decaying limestone in historical buildings at the Mamluks Cemetery - City of the Dead, Egypt. EJARS 9(2), 183-196. DOI: 10.21608/ejars.2019.66989.

537 Abu-Allaban, M., Lowenthal, D.H., Gertler, A.W., Labib, M., 2007. Sources of PM10 and PM2.5 in
538 Cairo's ambient air. Environ. Monit. Assess 133, 417–425. https://doi.org/10.1007/s10661-006-9596-8.
539 Abu-Allaban, M., Lowenthal, D.H., Gertler, A.W., Labib, M., 2009. Sources of volatile organic
540 compounds in Cairo's ambient air. Environ. Monit. Assess. 157, 179–189.
541 DOI 10.1007/s10661-008-0526-9.
542 Ahmed, H., Torok, A., Locsei, J., 2006. Performance of some commercial consolidating agents on
543 porous limestones from Egypt "Tura and Mokattam Quarry". In: Heritage, Weathering and Conservation:
544 Proceedings of the International Heritage, Weathering And Conservation Conference (HWC-2006), 21-24
545 June 2006 Madrid, Spain, pp. 735-740.
546 Alkhdhairi, S.A., Abdel-Hameed, U.K., Morsy, A.A., Tantawy, M.E., 2018. Air Pollution and its
547 Impact on the Elements of Soil and Plants in Helwan Area. Int. J. Adv. Res. Biol. Sci. 5(6), 38-59
548 http://dx.doi.org/10.22192/ijarbs.2018.05.06.004.
549 Aly, N., Hamed, A., Gomez-Heras, M., Alvarez de Buergo, M., 2015. The influence of temperature
550 in a capillary imbibition salt weathering simulation test on Mokkattam limestone. Mater. Construc. 65 (317).
551 https://doi.org/10.3989/mc.2015.00514.
552 Aly, N., Hamed, A., Abd El-Al, A., 2020. The impact of hydric swelling on the mechanical behavior
553 of Egyptian Helwan Limestone. Period. Polytech. Civ. 64(2), 589-596. https://doi.org/10.3311/PPci.15360.
554 Atzei, D., Fantauzzi, M., Rossi, A., Fermo, P., Piazzalunga, A., Valli, G., Vecchi, R., 2014. Surface
555 chemical characterization of PM10 samples by XPS. Appl. Surf. Sci. 307, 120-128.
556 https://doi.org/10.1016/j.apsusc.2014.03.178.
557 Barca, D., Belfiore, C.M., Crisci, G.M., La Russa, M.F., Pezzino, A., Ruffolo, S.A., 2011. A new
558 methodological approach for the chemical characterization of black crusts on building stones: a case study
559 from the Catania city centre (Sicily, Italy). J. Anal. At. Spectrom. 26, 1000–1011.
560 https://doi.org/10.1039/C0JA00226G.
561 Belfiore, C.M., Barca, D., Bonazza, A., Comite, V., La Russa, M.F., Pezzino, A., Ruffolo, S.A.,
562 Sabbioni, C., 2013. Application of spectrometric analysis to the identification of pollution sources causing
563 cultural heritage damage. Environ. Sci. Pollut. Res. 20, 8848–59. https://doi.org/10.1007/s11356-013-1810-
564 y.

Belis, C.A., Cancelinha, J., Duane, M., Forcina, V., Pedroni, V., Passarella, R., Tanet, G., Douglas, K., Piazzalunga, A., Bolzacchini, E., Sangiorgi, G., Perrone, M.G., Ferrero, L., Fermo P., Larsen, B.R., 2011. Sources for PM air pollution in the Po Plain, Italy: I. Critical comparison of methods for estimating biomass burning contributions to benzo(a) pyrene. Atmos. Environ. 45(39), 7266–7275. https://doi.org/10.1016/j.atmosenv.2011.08.061.

Bernardoni, V., Vecchi, R., Valli, G., Piazzalunga, A., Fermo P., 2011. PM10 source apportionment in Milan (Italy) using time-resolved data. Sci. Tot. Environ. 409, 4788–4795. https://doi.org/10.1016/j.scitotenv.2011.07.048.

Böke, H., Göktürk, E.H., Caner-Saltık, E.N., Demircia, Ş.,1999. Demirci Effect of airborne particle on SO –calcite reaction. Appl. Surf. Sci. 140 (1-2), 70–82. https://doi.org/10.1016/S0169-4332(98)00468-1.

Borai, E.H., Soliman, A.A., 2001. Monitoring and statistical evaluation of heavy metals in airborne particulates in Cairo, Egypt. J. Chromatogr. A. 920(1-2), 261-269. https://doi.org/10.1016/S0021-9673(01)00857-3.

Bove, M.C., Brotto, P., Calzolai, G., Cassola, F., Cavalli, F., Fermo, P., Hjorth, J., Massabò, D., Nava, S., Piazzalunga, A., Schembari, C., Prati P., 2016. PM10 source apportionment applying PMF and chemical tracer analysis to ship-borne measurements in the Western Mediterranean. Atmos. Environ. 125, 140-151. https://doi.org/10.1016/j.atmosenv.2015.11.009.

Bozzetti, C., El Haddad, I., Salameh, D., Daellenbach, K.R., Fermo, P., Gonzalez, R., Minguillón, M.C., Iinuma, Y., Poulain, L., Elser, M., Müller, E., Slowik, J.G., Jaffrezo, J.L., Baltensperger, U., Marchand, N., Prévôt, A.S.H., 2017. Organic aerosol source apportionment by offline-AMS over a full year in Marseille. Atmos. Chem. Phys. 17(13), 8247-8268. https://doi.org/10.5194/acp-17-8247-2017.

CAPMAS, 2017. Inventory of licensed vehicles for 2016. Cairo, Egypt: Central Agency for Public Mobilization and Statistics No. 71-21315-2016. https://www.capmas.gov.eg, last accessed: 18 June 2020.

Charola, A.E., 2000. Salts in the Deterioration of Porous Materials: An Overview. J. Am. Inst. Conservat. 39(3), 327-343. https://doi.org/10.1179/019713600806113176.

Chang, C.S., Rochelle, G.T., 1981. SO2 absorption into aqueous solutions. AIChE J. 27(2), 292–298.

Cheng, Z., Luo, L., Wang, S., Wang, Y., Sharma, S., Shimadera, H., Wang, X., Bressi, M., De Miranda, R.M., Jiang, J., Zhou, W., Fajardo, O., Yan, N., Hao, J., 2016. Status and characteristics of ambient

PM2.5 pollution in global megacities. Environ. Int. 89–90, 212–221. https://doi.org/10.1016/j.envint.2016.02.003.

Comite, V., Barca, D., Belfiore, C.M., Bonazza, A., Crisci, G.M., La Russa, M.F., Pezzino, A., Sabbioni, C., 2012. Potentialities of spectrometric analysis for the evaluation of pollution impact in deteriorating stone heritage materials. In: Rendiconti online della Società Geologica Italiana, 86 Congresso Nazionale della Società Geologica Italiana, Arcavacata di Rende, 18–20 September 2012, Roma, vol. 21, pp. 652–653.

Comite, V., Fermo, P., 2018. The effects of air pollution on cultural heritage: the case study of Santa Maria delle Grazie al Naviglio Grande (Milan). E.P.J. Plus. 133 (12), 556-566. https://doi.org/10.1140/epjp/i2018-12365-6.

Comite, V., Pozo-Antonio, J.S., Cardell, C., Rivas, T., Randazzo, L., La Russa, M.F., Fermo, P., 2019. Metals distributions within black crusts sampled on the facade of an historical monument: The case study of the Cathedral of Monza (Milan, Italy). In: IMEKO TC4 International Conference on Metrology for Archaeology and Cultural Heritage (MetroArchaeo), 04 - 06 December 2019, Florence, pp.73-78.

Comite, V., Ricca, M., Ruffolo, S.A., Graziano, S.F., Rovella, N., Rispoli, C., Gallo, C., Randazzo, L., Barca, D., Cappelletti, P., La Russa, M.F., 2020a. Multidisciplinary approach to evaluate the geochemical degradation of building stone related to pollution sources in the Historical Centre of Naples (Italy). Int. J. Conserv. Sci. 11(1), 291-304. https://doi.org/10.3390/app10124241.

Comite, V., Pozo-Antonio, J.S., Cardell, C., Rivas, T., Randazzo, L., La Russa, M.F., Fermo, P., 2020b. Environmental impact assessment on the Monza cathedral (Italy): a multi-analytical approach. Int. J. Conserv. Sci. 11(1), 291-304.

Comite, V., Pozo-Antonio, J.S., Cardell, C., Randazzo, L., La Russa, M.F., Fermo, P., 2020c. A multi-analytical approach for the characterization of black crusts on the facade of an historical cathedral. Microchem. J. 158, 105121. https://doi.org/10.1016/j.microc.2020.105121.

Creighton, P.J., Lioy, P.J., Haynie, F.H., Lemmons, T.J., Miller, J.L., Gerhart, J., 1990. Soiling by Atmospheric Aerosols in an Urban Industrial Area. J. Air Waste Manag. Assoc. 40(9), 1285-1289. https://doi.org/10.1080/10473289.1990.10466783.

620 Cultrone, G., Rodriguez-Navarro, C., Sebastian, E., 2004. Limestone and brick decay in simulated
621 polluted atmosphere: the role of particulate matter, in: Siaz-Jimenez, C. (Eds.), Air Pollution and Cultural
622 Heritage. Balkema A.A. Publishers, Leiden, London, New York, Philadelphia, Singapore, pp. 141–145.
623 Daellenbach, K.R., Bozzetti, C., Křepelová, A., Canonaco, F., Wolf, R., Zotter, P., Fermo, P.,
624 Crippa, M., Slowik, J.G., Sosedova, Y., Zhang, Y., Huang, R.J., Poulain, L., Szidat, S., Baltensperger, U., El
625 Haddad, I., Prévôt, A.S.H., 2016. Characterization and source apportionment of organic aerosol using offline
626 aerosol mass spectrometry. Atmos. Meas. Tech. 9(1), 23–39. https://doi.org/10.5194/amt-9-23-2016.
627 Davidson, C.I., Tang, F., Finger, S., Etyemezian, V., Sherwood, S.I., 2000. Soiling patterns on a tall
628 limestone building: changes over 60 years. Environ. Sci. Technol. 34(4), 560–565.
629 https://doi.org/10.1021/es990520y.
630 Dunham, R.J., (1962). Classification of carbonate rocks according to depositional textures. Amer.
631 Assoc. Petrol. Geol. Mem. 1, 108-121.
632
633 Duquennois, A.N., Newman, P., 2009. Linking the green and brown agendas: A case study on Cairo,
634 Egypt. UN habitat, global report on human settlements. http://www.unhabitat.org/grhs/2009, last accessed:
635 24 June 2020.
636 El-Dorghamy, A., Allam, H., Al-Abyad, A., Gasnier, M., 2015. Fuel economy and CO2 emissions of
637 light-duty vehicles in Egypt. Centre for Environment and Development in the Arab Region and Europe
638 (CEDARE). http://web.cedare.org/, last accessed: 20 June 2020.
639 El Mowafi, S.A., Atalla, A.G., 2005. Strategies for controlling mobile emissions in Cairo. Manag.
640 Environ. Qual. 16(5), 548-559. https://doi.org/10.1108/14777830510614385.
641 El-Nahhas, F., Moustafa, A., Abdel-Tawab, S., 1990. Geotechnical characteristics of limestone
642 formations of Gebel Mokattam area. Proceedings of First Alexandria Conference on Structural and
643 Geotechnical Engineering, Alexandria University, Egypt, vol. 1, pp. 9-19.
644 El-Tawab, N.A., Mahran, A., Badr, I., 2012. Restoration and preservation of the wooden ceiling of
645 Al-Ashraf Qaytbay madressa, Cairo Egypt. EJARS 2(1), 11-28. doi: 10.21608/ejars.2012.7456
646 El-Mansy, A., Heikal, A., Abo Taleb A., 2013. Integration of GPS and GIS to study traffic
647 congestion on Cairo Road network to minimize the harmful environmental effects. Case study (autostrad

Road). Partial fulfilment of the requirement for the master degree. Cairo Egypt: Ain Shams University, Lambert Academic Publishing, Cairo.

Favez, O., Cachiera, H., Sciare, J., Alfaro, S.C., El-Araby, T.M., Harhash, M.A., Abdelwahab, M.M., 2008. Seasonality of major aerosol species and their transformations in Cairo megacity. Atmos. Environ. 42, 1503–1516. https://doi.org/10.1016/j.atmosenv.2007.10.081.

Fermo, P., Turrion, R.G., Rosa, M., Omegna, A., 2015. A new approach to assess the chemical composition of powder deposits damaging the stone surfaces of historical monuments. Environ. Sci. Pollut. Res. 22, 6262-6270. https://doi.org/10.1007/s11356-014-3855-y.

Fermo, P., Comite, V., Ciantelli, C., Sardella, A., Bonazza, A., 2020. A multi-analytical approach to study the chemical composition of total suspended particulate matter (TSP) to assess the impact on urban monumental heritage in Florence. Sci. Total. Environ. 740-140055.

Fitzner, B., Heinrichs, K., La Bouchardiere, D., 2002. Weathering damage on Pharaonic sandstone monuments in Luxor-Egypt. Build Environ 38, 1089-1103. DOI: 10.1016/S0360-1323(03)00086-6.

Folk, R.L., 1959. Practical petrographic classification of limestones. Bull. Amer. Assoc. Petrol. Geol. 43, 1-38. https://doi.org/10.1306/0BDA5C36-16BD-11D7-8645000102C1865D.

Fujiwara, F., Rebagliati, R.J., Dawidowski, L., Gómez, D., Polla, G., Pereyra, V., Smichowski, P., 2011. Spatial and chemical patterns of size fractionated road dust collected in a megacity. Atmos. Environ. 45, 1497-1505. https://doi.org/10.1016/j.atmosenv.2010.12.053.

Fuzzi, S., Andreae, M.O., Hueber, B.J., Kulmala, M., Bon, T.C., Boy, M., Doherty, S.J., Guenther, A., Kanakidou, M., Kawamura, K., Kerminen, V.M., Lohmann, U., Russell, L.M., Poschl, U., 2006. Critical assessment of the current state of scientific knowledge, terminology, and research needs concerning the role of organic aerosols in the atmosphere, climate, and global change. Atmos. Chem. Phys. 6, 2017–2038. https://doi.org/10.5194/acp-6-2017-2006.

Gallego, J.R., Ortiz, J.E., Sierra, C., Torres, T., Llamas, J.F., 2013. Multivariate study of trace element distribution in the geological record of Roñanzas Peat Bog (Asturias, N. Spain). Palaeoenvironmental evolution and human activities over the last 8000 cal yr BP. Sci. Total Environ. 454, 16-29. https://doi.org/10.1016/j.scitotenv.2013.02.083.

675 Gao, S., Liu, X., Yuan, H., Hattendorf, B., Gunther, D., Chen, L., Hu, S., 2002. Determination of
676 forty two major and trace elements in USGS and NIST SRM glasses by laser ablation-inductively coupled
677 plasma mass spectrometry. Geostandard Newslett. 26, 181–196. https://doi.org/10.1111/j.1751-
678 908X.2002.tb00886.x.
679 Gauri, K.L., Holdren, G.C., 1981. Deterioration of the stone of the Great Sphinx. ARCE Newsletter,
680 114, 35-47.
681 Gauri, K.L., Holdren, G.C., Vaughan, W.C., 1986. Cleaning Efflorescences from Masonry, in:
682 Clifton, J.R. (ed.), Cleaning Stone and Masonry. American Society for Testing and Materials, Philadelphia,
683 pp. 3-13.
684 Gentner, D.R., Isaacman, G., Worton, D.R., Chan, A.W.H., Dallmann, T.R., Davisa, L., Liud, S.,
685 Day, D.A., Russell, L.M., Wilson, K.R., Weber, R., Guha, A., Harley, R.A., Goldstein, A.H., 2012.
686 Elucidating secondary organic aerosol from diesel and gasoline vehicles through detailed characterization of
687 organic carbon emissions. Proc. Natl. Acad. Sci. U.S.A. 109, 18318–18323.
688 https://doi.org/10.1073/pnas.1212272109.
689 Ghedini, N., Gobbi, G., Sabbioni, C., Zappia, G., 2000. Determination of elemental and organic
690 carbon on damaged stone monuments. Atmos. Environ. 34(25), 4383-4391. https://doi.org/10.1016/S1352-
691 2310(00)00250-8.
692 Gomez-Heras, M., Fort, R., 2007. Patterns of halite (NaCl) crystallisation in building stone
693 conditioned by laboratory heating regimes. Environ. Geol. 52, 259–267. https://doi.org/10.1007/s00254-006-
694 0538-0.
695 Graue, B., Siegesmund, S., Oyhantcabal, P., Naumann, R., Licha, T., Simon, K., 2013. The effect of
696 air pollution on stone decay: the decay of the Drachenfels trachyte in industrial, urban, and rural
697 environments—a case study of the Cologne, Altenberg and Xanten cathedrals. Environ. Earth Sci. 69, 1095–
698 1124. https://doi.org/10.1007/s12665-012-2161-6.
699 Gundel, L.A., Guyot-Sionnest, N.S., Novakov, T., 1989. A study of the interaction of NO_2 with
700 carbon particles. Aerosol Sci. Tech. 10(2), 343-351. https://doi.org/10.1080/02786828908959271.

Gunther, D., Heinrich, C.A., 1999. Enhanced sensitivity in laser ablation-ICP mass spectrometry using helium–argon mixtures as aerosol carrier. J. Anal. At. Spectrom. 14, 1363–1368. https://doi.org/10.1039/A901648A

Gurjar, B.R., Nagpure, A.S., Singh, T.P., Hanson, H., 2010. Air quality in megacities, in: Cleveland, C.J. (Eds.), Encyclopedia of Earth. Environmental Information Coalition, National Council for Science and the Environment. Washington D.C. http://www.eoearth.org/article/Air_quality_in_mega cities.

Helmi, F.M., 1990. Study of salt problem in the sphinx, Giza, Egypt. In: 9th Triennial meeting, ICOM Committee for Conservation, 26-31 August 1990, vol.1, Dresden, Germany. Grimstad, K. (Ed.), ICOM Committee for Conservation, Los Angeles, pp. 326-329.

Johnson, C.C., Demetriades, A., Locutura, J., Ottesen, R.T., 2011. Mapping the Chemical Environment of Urban Areas. Wiley, New York City, United States, ISBN: 978-0-470-74724-7, 640 Pages.

Kanakidou, M., Mihalopoulos, N., Kindap, T., Im, U., Vrekoussis, M., Gerasopoulos, E., Dermitzaki, E., Unal, A., Koçak, M., Markakis, K., Melas, D., Kouvarakis, G., Youssef, A.F., Richter, A., Hatzianastassiou, N., Hilboll, A., Ebojie, F., Wittrock, F., von Savigny, C., Burrows, J.P., Ladstaetter-Weissenmayer, A., Moubasher. H., 2011. Review Megacities as hot spots of air pollution in the East Mediterranean. Atmos. Environ. 45(6), 1223-1235. https://doi.org/10.1016/j.atmosenv.2010.11.048.

Khairy, M.A., Barakat, A.O., Mostafa, A.R., Wade, T.L., 2011. Multielement determination by flame atomic absorption of road dust samples in Delta Region, Egypt. Microchem. J. 97(2), 234-242. https://doi.org/10.1016/j.microc.2010.09.012.

Khallaf, M.K., 2011. Effect of Air Pollution on Archaeological Buildings in Cairo, in: Chmielewski, A. (Eds.), Monitoring, Control and Effects of Air Pollution. IntechOpen, London, pp. 179-200. https://doi.org/10.5772/16748.

Köppen, W., Geiger R., 1930. Handbuch der Klimatologie, Gebrueder Borntraeger (Eds.), Berlin.

Kukela, A., Segliņš, V., 2011. Simplified Method of Assessment of Weathering on Historical Stone Monuments: An Example of El-Merdani Mosque, Cairo, Egypt. J. Earth Sci. Eng. 1, 82-90.

La Russa, M.F., Ruffolo, S.A., Belfiore, C.M., Aloise, P., Randazzo, L., Rovella, N., Pezzino, A., Montana, G., 2013a. Study of the effects of salt crystallization on degradation of limestone rocks. Period. Mineral. 82(1), 113-127. http://dx.doi.org/10.2451/2013PM0007.

La Russa, M.F., Belfiore, C.M., Comite, V., Barca, D., Bonazza, A., Ruffolo, S.A., Crisci, G.M., Pezzino, A., 2013b. Geochemical study of black crusts as a diagnostic tool in cultural heritage. Appl. Phys. A Mater. 113, 1151–62. https://doi.org/10.1007/s00339-013-7912-z.

La Russa, M.F., Fermo, P., Comite, V., Belfiore, C.M., Barca, D., Cerioni, A., De Santis, M., Barbagallo, L.F., Ricca, M., Ruffolo, S. A., 2017. The Oceanus statue of the Fontana di Trevi (Rome): The analysis of black crust as a tool to investigate the urban air pollution and its impact on the stone degradation. Sci. Total. Environ., 593-594, 297-309. https://doi.org/10.1016/j.scitotenv.2017.03.185.

La Russa, M.F., Comite, V., Aly, N., Barca, D., Fermo, P., Rovella, N., Antonelli, F., Tesser, E., Aquino, M., Ruffolo, S.A., 2018. Black crusts on Venetian built heritage, investigation on the impact of pollution sources on their composition. Eur. Phys. J. Plus 133, 370. https://doi.org/10.1140/epjp/i2018-12230-8.

Loring, D.H., 1991. Normalization of heavy-metal data from estuarine and coastal sediments. ICES J. Mar. Sci. 48(1), 101-115. https://doi.org/10.1093/icesjms/48.1.101.

Lowenthal, D.H., Gertler, A.W., Labib, M.W., 2014. Particulate matter source apportionment in Cairo: recent measurements and comparison with previous studies. Int. J. Environ. Sci. Technol. 11 (3), 657–670. https://doi.org/10.1007/s13762-013-0272-6.

Mahmoud, K.F., Alfaro, S.C., Favez, O., Abdel Wahab, M.M., Sciare, J., 2018. Origin of black carbon concentration peaks in Cairo (Egypt). Atmos. Res. 89 (1-2), 161–169. https://doi.org/10.1016/j.atmosres.2008.01.004.

McAlister, J.J., Smitha, B.J., Tőrők, A., 2008. Transition metals and water-soluble ions in deposits on a building and their potential catalysis of stone decay. Atmos. Environ. 42 (33), 7657–68. https://doi.org/10.1016/j.atmosenv.2008.05.067.

Mostafa, A.N., Zakey, A.S., Monem, A.S., Wahab M.M.A., 2018. Analysis of the surface air quality measurements in the Greater Cairo (Egypt) metropolitan. GJAR, 5(6), 207–214.

Orphy, M., Hamid, A., 2004. Problems Islamic monuments in Cairo face. In: 13th International Brick and Block Masonry Conference Amsterdam, July 4-7, 2004. Martens, D.R.W., Vermeltfoort, A.T. (Eds). Eindhoven: Technische Universiteit Eindhoven.

Park, H.D., Shin, G.H., 2009. Geotechnical and geological properties of Mokattam limestones: Implications for conservation strategies for ancient Egyptian stone monuments. Eng. Geol. 104(3–4),190-199. https://doi.org/10.1016/j.enggeo.2008.10.009

Pearce, N.J.G., Perkins, W.T., Westgate, J.A., Gorton, M.P., Jackson, S.E., Neal, C.R., Chenery, S.P., 1997. A compilation of new and published major and trace element data for NIST SRM 610 and NIST SRM 612 glass reference materials. Geostandard Newslett. 21, 115–144. https://doi.org/10.1111/j.1751-908X.1997.tb00538.x.

Perrino, C., Canepari, S., Catrambone, M., Dalla Torre, S., Rantica, E., Sargolini, T., 2009. Influence of natural events on the concentration and composition of atmospheric particulate matter. Atmos. Environ. 43, 4766–4779. https://doi.org/10.1016/j.atmosenv.2008.06.035.

Piazzalunga, A., Fermo, P., Bernardoni, V., Vecchi, R., Valli, G., De Gregorio, M., 2010. A simplified method for levoglucosan quantification in wintertime atmospheric particulate matter by high performance anion-exchange chromatography coupled with pulsed amperometric detection. Int. J. Environ. Anal. Chem. 90, 934–947. http://dx.doi.org/10.1080/03067310903023619.

Piazzalunga, A., Belis C., Bernardoni, V., Cazzuli, O., Fermo, P., Valli, G., Vecchi, R., 2011. Estimates of wood burning contribution to PM by the macro-tracer method using tailored emission factors. Atmos. Environ. 45, 6642–6649. https://doi.org/10.1016/j.atmosenv.2011.09.008.

Pio, C.A., Legrand, M., Oliveira, T., Afonso, J., Santos, C., Caseiro, A., Fialho, P., Barata, F., Puxbaum, H., Sanchez-Ochoa, A., Kasper-Giebl, A., Gelencser, A., Preunkert, S., Schock, M., 2007. Climatology of aerosol composition (organic versus inorganic) at nonurban sites on a west-east transect across Europe. J. Geophys. Res.-Atmos. 112, 1-15. https://doi.org/10.1029/2006JD008038.

Reimann, C., Caritat, P., 2000. Intrinsic flaws of element enrichment factors (EFs) in environmental geochemistry. Environ. Sci. Technol. 34(24), 5084–5091. https://doi.org/10.1021/es001339o.

Ricca, M., Le Pera, E., Licchelli, M., Macchia, A., Malagodi, M., Randazzo, L., Rovella, N., Ruffolo, S.A., Weththimuni, M.L., La Russa, M.F., 2019. The CRATI Project: New Insights on the Consolidation of Salt Weathered Stone and the Case Study of San Domenico Church in Cosenza (South Calabria, Italy). Coatings 9, 330-345. https://doi.org/10.3390/coatings9050330.

Robaa, S.M., 2003. Urban–suburban/rural differences over Greater Cairo, Egypt. Atmosfera 16, 157–171.

Robinson, A.L., Donahue, N.M., Shrivastava, M.K., Weitkamp, E.A., Sage, A.M., Grieshop, A.P., Lane, T.E., Pierce, J.R., Pandis, S.N., 2007. Rethinking Organic Aerosols: Semivolatile Emissions and Photochemical Aging. Science 315(5816), 1259-1262. https://doi.org/10.1126/science.1133061.

Rodriguez-Navarro, C., Sebastian, E., 1996. Role of particulate matter from vehicle exhaust on porous building stones (limestone) sulfation. Sci. Total Environ. 187, 79–91. https://doi.org/10.1016/0048-9697(96)05124-8.

Rovella, N., Aly, N., Comite, V., Ruffolo, S.A., Ricca, M., Fermo, P., Alvarez De Buergo, M., La Russa, M.F., 2020. A Methodological approach to define the state of conservation of the stone materials used in the Cairo historical heritage (Egypt). Archaeol. Anthrop. Sci. in press. https://doi.org/ 10.1007/s12520-020-01126-x.

Ruffolo, S.A., Comite, V., La Russa, M.F., Belfiore, C.M., Barca, D., Bonazza, A., Crisci, G.M., Pezzino, A., Sabbioni, C., 2015. An analysis of the black crusts from the Seville Cathedral: A challenge to deepen the understanding of the relationships among microstructure, microchemical features and pollution sources. Sci. Total Environ. 502, 157-166, https://doi.org/10.1016/j.scitotenv.2014.09.023.

Saarikoski, S., Timonen, H., Saarnio, K., Aurela, M., Jarvi, L., Keronen, P., Kerminen, V.M., Hillamo, R., 2008. Sources of organic carbon in fine particulate matter in northern European urban air. Atmos. Chem. Phys. 8, 6281-6295. https://doi.org/10.5194/acp-8-6281-2008.

Sanjurjo Sánchez, J., Vidal Romaní, J.R., Alves, C., 2011. Deposition of particles on gypsum-rich coatings of historic buildings in urban and rural environments. Constr. Build. Mater. 25, 813–822. https://doi.org/10.1016/j.conbuildmat.2010.07.001.

Schauer, J.J., Kleeman, M., Cass, G., Simoneit, B.R., 1999. Measurement of emissions from air pollution sources. 1. C1 through C29 organic compounds from meat charbroiling. Environ. Sci. Technol. 33(10), 1566–1577. https://doi.org/10.1021/es980076j.

Schauer, J.J., Kleeman, M.J., Cass, G.R., Simoneit, B.R., 2002. Measurement of emissions from air pollution sources. 5. C1-C32 organic compounds from gasoline-powered motor vehicles. Environ. Sci. Technol. 36, 1169–1180. http://dx.doi.org/10.1021/es0108077.

Shaltout, A.A., Welz, B., Castilho, I.N.B., 2013a. Determination of Sb and Mo in Cairo's dust using high resolution continuum source graphite furnace atomic absorption spectrometry and direct solid sample analysis. Atmos. Environ. 81, 18–24. http://dx.doi.org/10.1016/j.atmosenv.2013.08.049.

Shaltout, A.A., Khoder, M.I., El-Abssawy, A.A., Hassan, S.K., Borges, D.L.G., 2013b. Determination of rare earth elements in dust deposited on tree leaves from Greater Cairo using inductively coupled plasma mass spectrometry, Environ. Pollut. 178, 197–201. http://dx.doi.org/10.1016/j.envpol.2013.03.044.

Shaltout, A.A., Boman, J., Welz, B., Castilho, I.N.B., Al Ashkar, E.A., Gaita, S.M., 2014. Method development for the determination of Cd, Cu, Ni and Pb in PM2.5 particles sampled in industrial and urban areas of Greater Cairo, Egypt, using high-resolution continuum source graphite furnace atomic absorption spectrometry. Microchem. J. 113, 4–9. https://doi.org/10.1016/j.microc.2013.10.009.

Simaõ, J., Ruiz-Agudo, E., Rodriguez-Navarro, C., 2006. Effects of particulate matter from gasoline and diesel vehicle exhaust emissions on silicate stones sulfation. Atmos. Environ. 40, 6905–6917. https://doi.org/10.1016/j.atmosenv.2006.06.016.

Tidblad, J., Kucera, V., Ferm, M., Kreislova, K., Brüggerhoff, S., Doytchinov, S., Screpanti, A., Grøntoft, T., Yates, T., De La Fuente, D., Roots, O., Lombardo, T., Simon, S., Faller, M., Kwiatkowski, L., Kobus, J., Varotsos, C., Tzanis, C., Krage, L., Schreiner, M., Melcher, M., Grancharov, I., Karmanova, N., 2012. Effects of air pollution on materials and cultural heritage: ICP materials celebrates 25 years of research. Int. J. Corros. 1-16. https://doi.org/10.1155/2012/496321.

Török, Á., Licha, T., Simon, K., Siegesmund, S., 2011. Urban and rural limestone weathering; the contribution of dust to black crust formation. Environ. Earth Sci. 63, 675–693. https://doi.org/10.1007/s12665-010-0737-6.

Vassura, I., Venturini, E., Marchetti, S., Piazzalunga, A., Bernardi, E., Fermo, P., Passarini, F., 2014. Markers and influence of open biomass burning on atmospheric particulate size and composition during a major bonfire event. Atmos. Environ. 82, 218–225. https://doi.org/10.1016/j.atmosenv.2013.10.037.

Wahba, M.M., Zaghloul, A.M., 2007. Adsorption characteristic of some heavy metals by some soil minerals. Res. J. Appl. Sci. 3(6), 421 – 426.

838 Whalley, B., Smith, B., Magee, R., 1992. Effects of particular air pollutants on materials:
839 investigation of surface crust formation. In: Stone cleaning and the nature, soiling and decay mechanisms of
840 stone: proceedings of the international conference held in Edinburgh, UK, 14-16 April 1992, pp. 227-234.
841 Williams, C., 2002. Islamic Monuments in Cairo: The Practical Guide. The American University in
842 Cairo Press, Cairo.
843 Zakey, A.S., Wahab, M.A., Pettersson, J.B.C., Gatari, M.J., Hallquist, M., 2008. Seasonal and spatial
844 variation of atmospheric particulate matter in a developing megacity, the Greater Cairo, Egypt. Atmósfera
845 21(2), 171-189.
846
847
848
849
850
851
852
853
854
855
856
857
858
859
860
861
862
863

Caption Figures

Fig. 1. Microphotographs obtained by OM observations highlighting the main textural features of the limestones and the overlaying black crusts. The red dashed lines mark the contact substrate/crust. Each image is relative to a different sample at 5X magnification. a) sample 2 (Crossed Polarized Light view - CPL). b) Sample 14 (Plane Polarized Light view – PPL). c) Sample 15 (CPL). d) Sample E (CPL). e) Sample H (CPL).

Fig. 2. EFs of black crusts from Salah El Din Citadel and Magra El-Oyoun sampling sites, Qaitbay Mosque, Sultan Faraj ibn Barquq Mosque and Qansuh Al-Ghuri Mausoleum sampling sites.

Fig. 3. Box plot variations of heavy metal concentrations in black crusts samples.

Fig. 4. Graph of the OC and EC concentrations (wt.%) obtained from the analysis of the black crust samples in relation to the sampling height for each site. The monuments of the entire Cairo data set are: a) Al Manial Palace; b) Magra El-Oyoun wall; c) Salah El Din citadel; d) Tower of Bab Al Azab; e) Qaitbay Mosque; f) Sultan Faraj ibn Barquq Mosque (collection of a new sample 15), g) Quansuh Al-Ghury Mausoleum; h) Al Silahdar Mosque.
* after Rovella et al. (2020).

Fig 5. a) EC vs OC binary diagram of the crust samples analysed by the different monuments in Cairo (this work and after Rovella et al., 2020); b) map of the city of Cairo where the different monuments are located.

Fig. 6. a) Binary diagram OC vs EC of the analysed black crusts. b) Histogram of the average OC/EC ratios of the analyzed black crust from the Cairo city (this work and after Rovella et al., 2020). Literature data used for the comparison refer to the crust samples taken from Cairo after Rovella et al., 2020; from the Trevi Fountain in Rome (La Russa et al., 2017); from several private buildings in Venice (La Russa et al., 2018), from the Church of Santa Maria delle Grazie in Milan (Comite and Fermo, 2018) and from the Cathedral of Monza located in the homonymous city (Comite at al., 2020).

Table

Click here to download Table: Table 1.docx

Table 1 Information about samples in terms of position and age of construction (William, 2004). They consist of both black crust and limestone substrate.

Monument	Sample ID	Position	Height of sampling
Salah El Din citadel (1176-1183)	2	Western walls	1 m
	3		1,90 m
Magra El-Oyoun (1193)	12	Western walls	2,5 m
	14		1,3 m
Sultan Faraj ibn Barquq Mosque (1400-1411)	15	Main Facade	2,5 m
Qaitbay Mosque (1472-1474)	B	Main Facade	0,80 m
	E		1,0 m
Qansuh Al-Ghuri Mausoleum (1503-1505)	H	Main Facade	1,8 m

Table

Click here to download Table: Table 2.docx

Table 2 TC (Total Carbon), OC (Organic Carbon), EC (Elemental Carbon) OX (Oxalate) CC (Carbonate Carbon) Gy (Gypsum) concentrations (wt%); and OC/EC and EC/TC ratio

Sample	TC	OC	EC	OX	CC	Gy	OC/EC	EC/TC
2	7.4	0.87	2.83	0.28	3.70	8.45	0.31	0.38
3	6.61	1.22	1.53	0.14	3.72	22.63	0.75	0.23
14	6.65	0.96	2.40	0.15	3.14	25.55	0.40	0.36
12	5.43	0.75	1.45	0.22	3.01	51.25	0.52	
15	5.11	0.66	1.23	0.11	3.11	15.01	0.54	0.24
B	7.88	0.99	1.48	1.15	4.26	32.98	0.23	0.19
E	6.41	1.36	2.15	0.15	2.75	9.57	0.49	0.34
H	7.75	1.12	1.99	0.09	4.55	9.57	0.25	0.26

Figure
Click here to download high resolution image

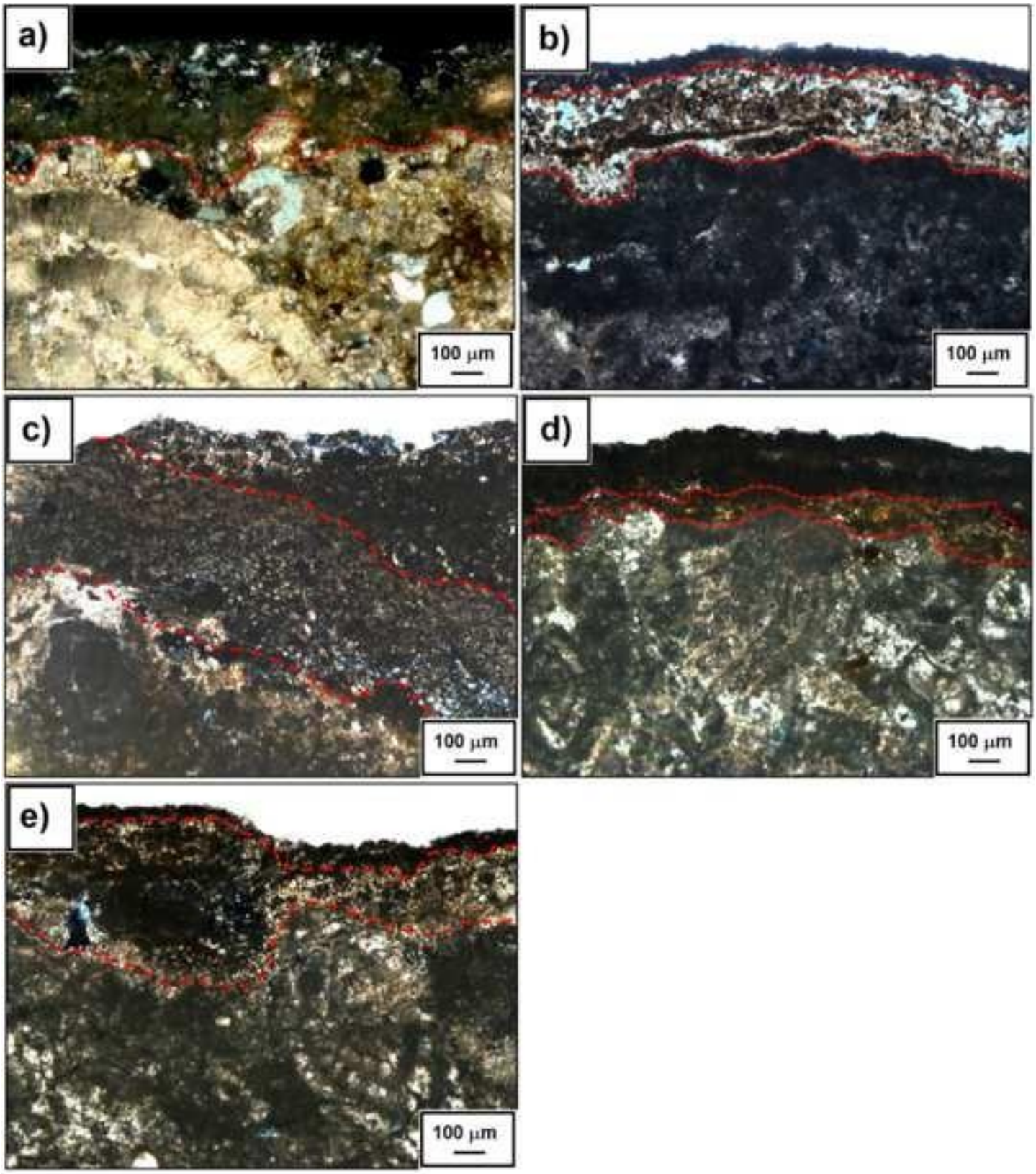

Figure

Click here to download high resolution image

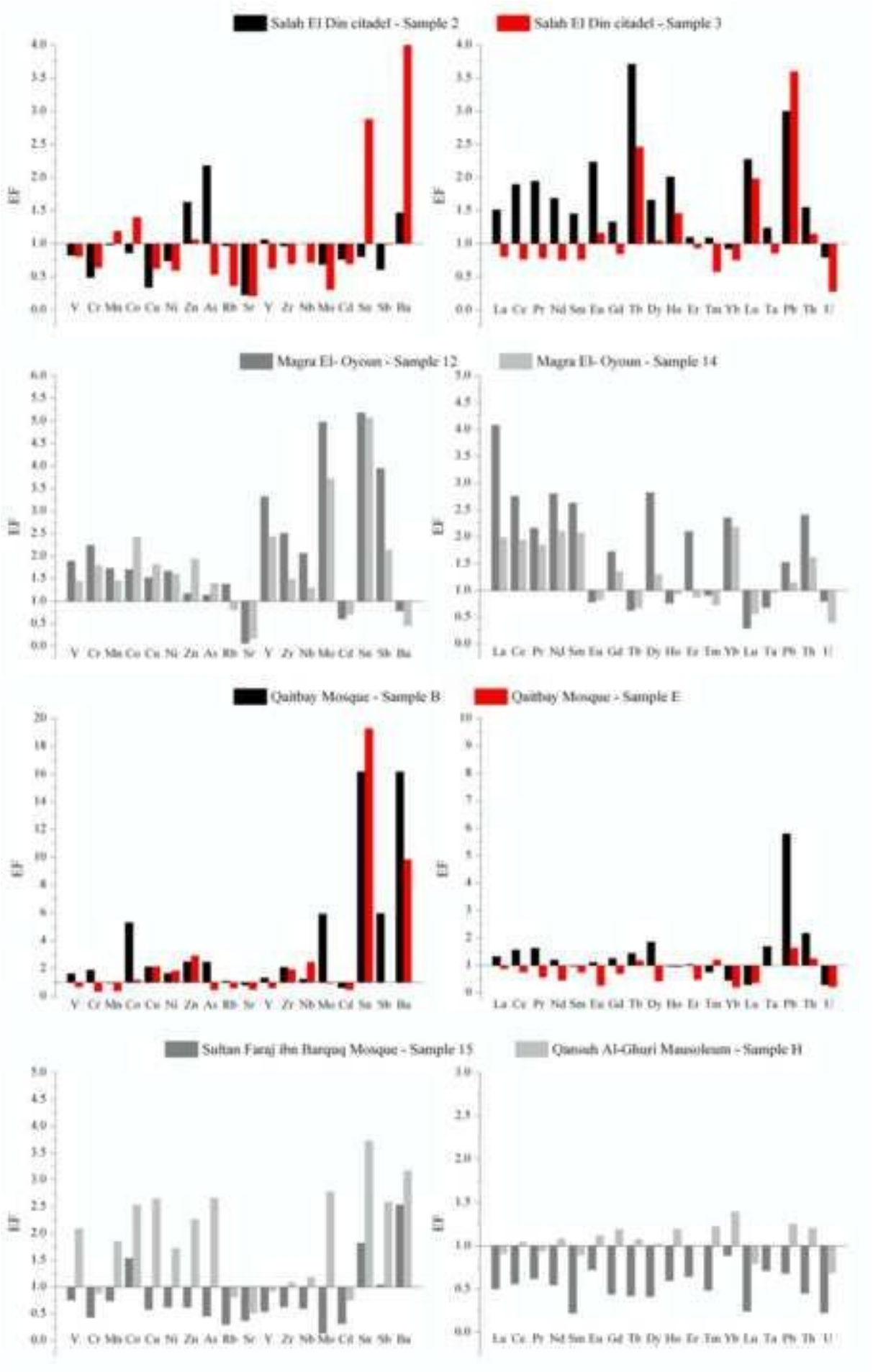

Figure

Click here to download high resolution image

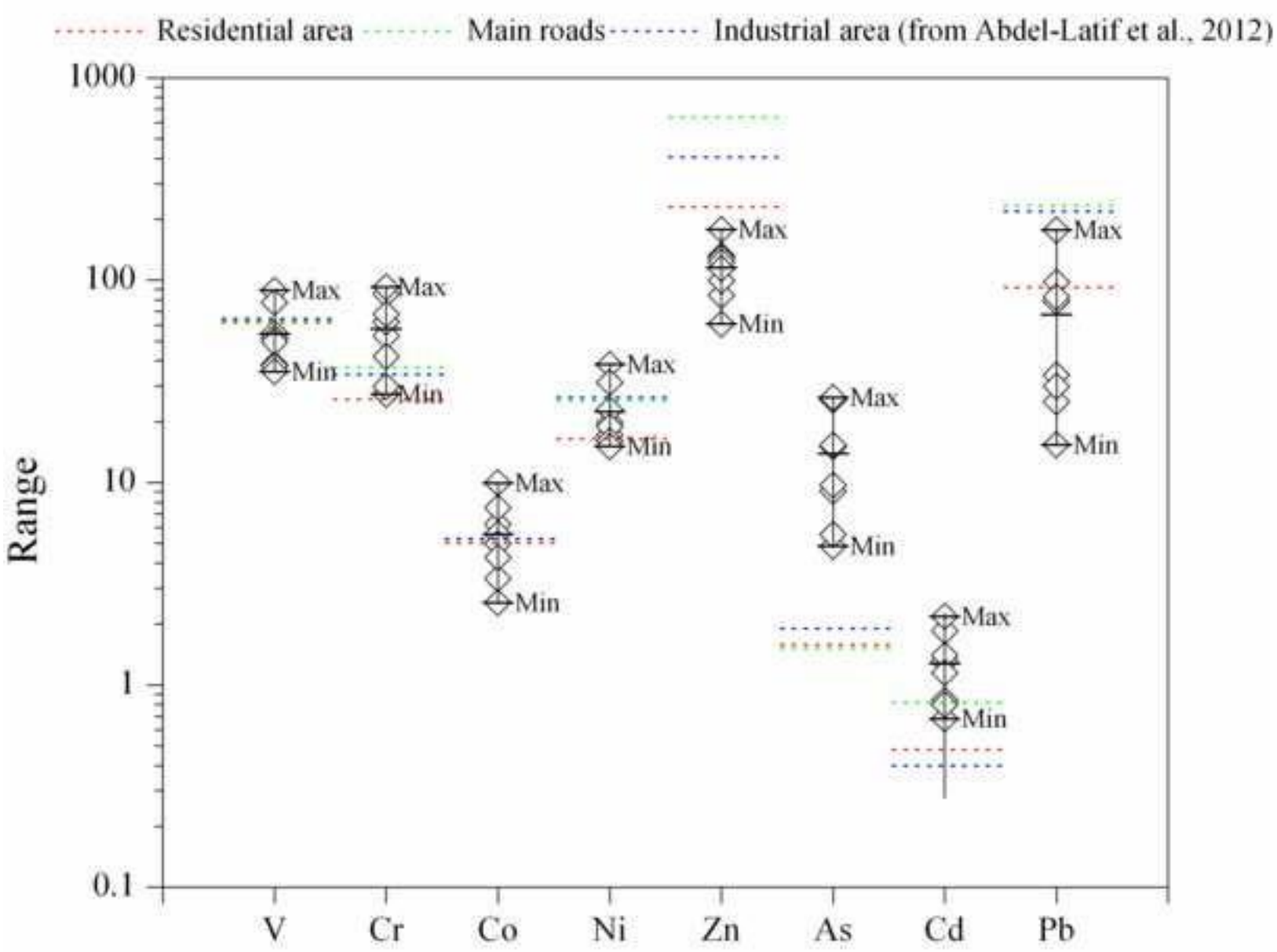

Figure

Click here to download high resolution image

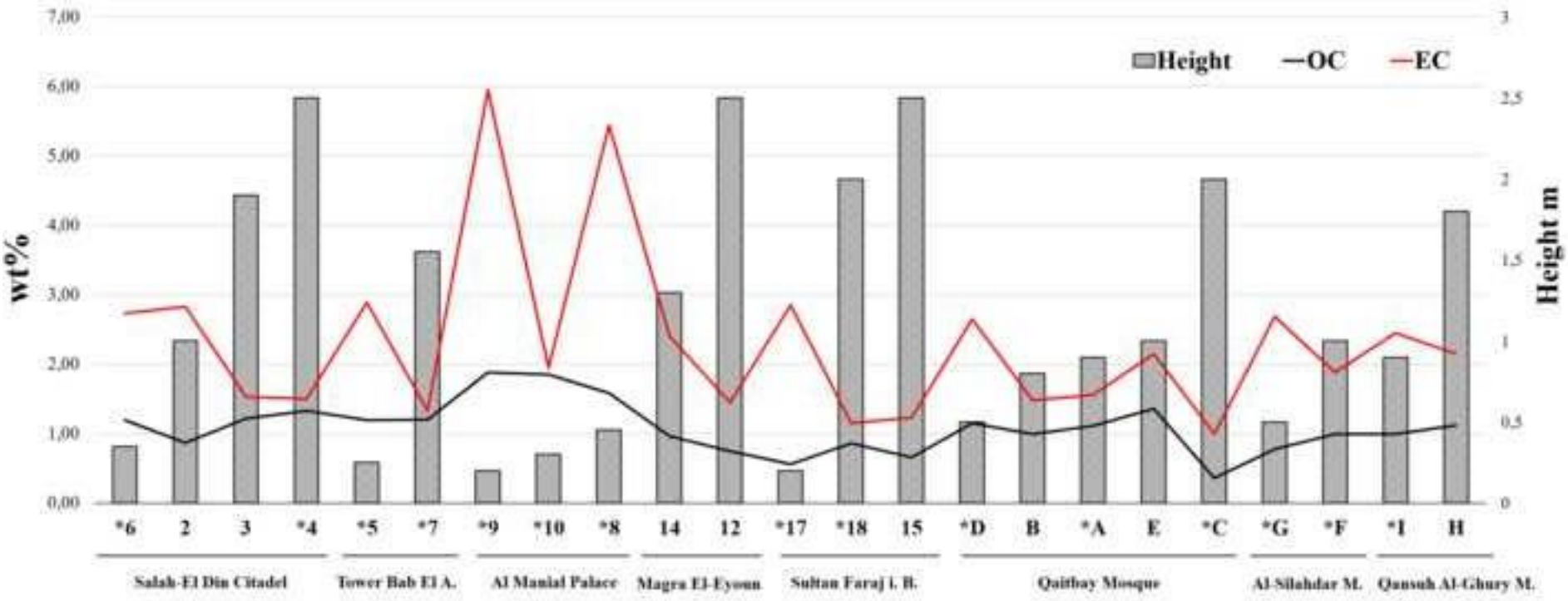

Figure

Click here to download high resolution image

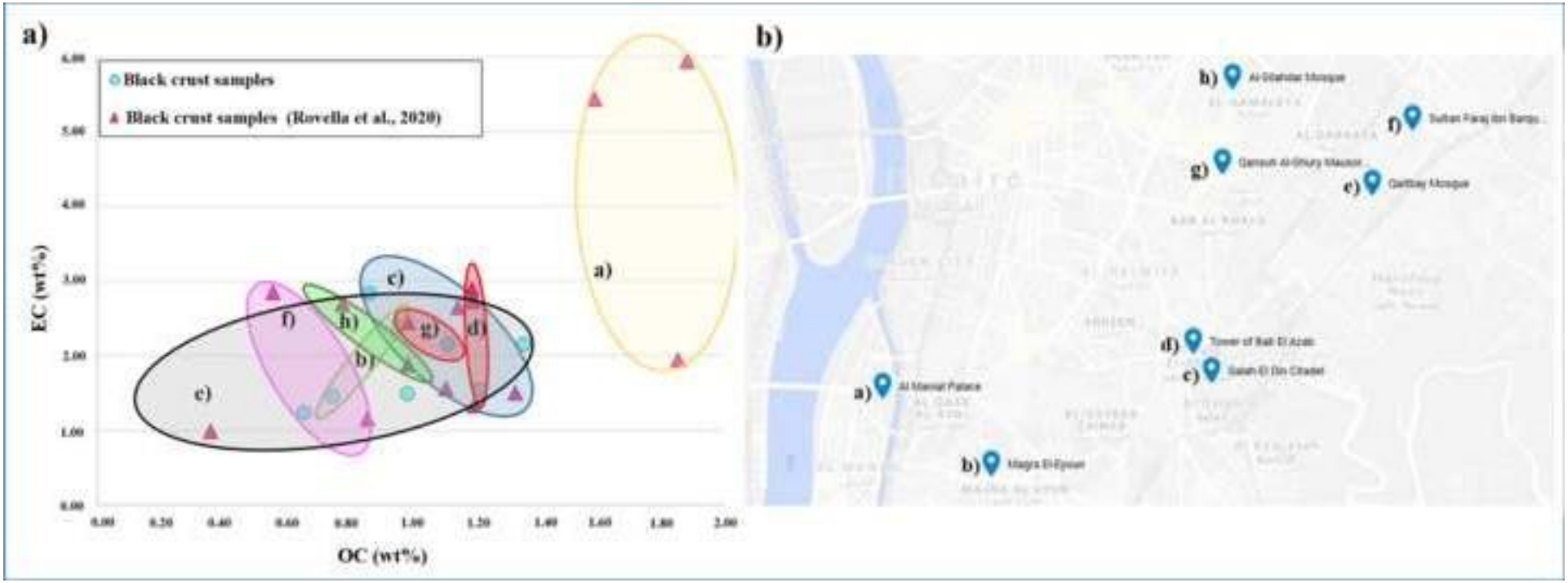

Figure

Click here to download high resolution image

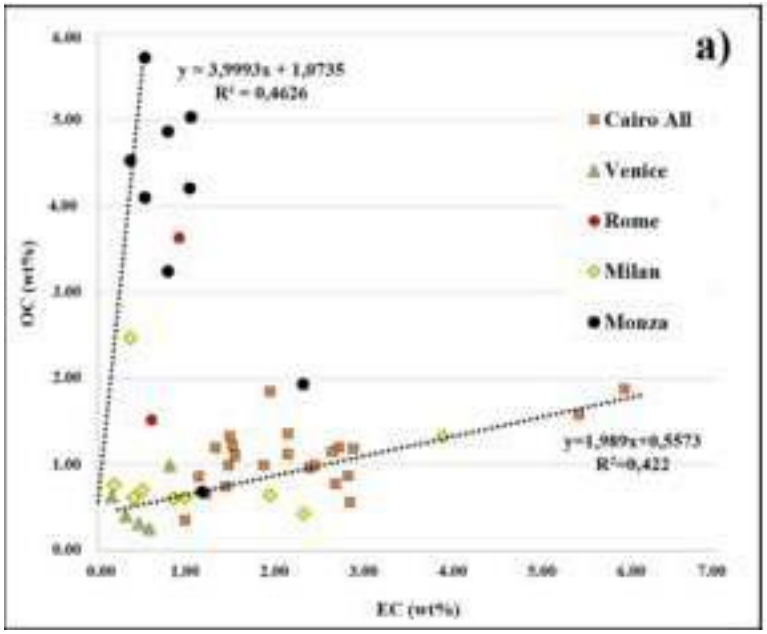

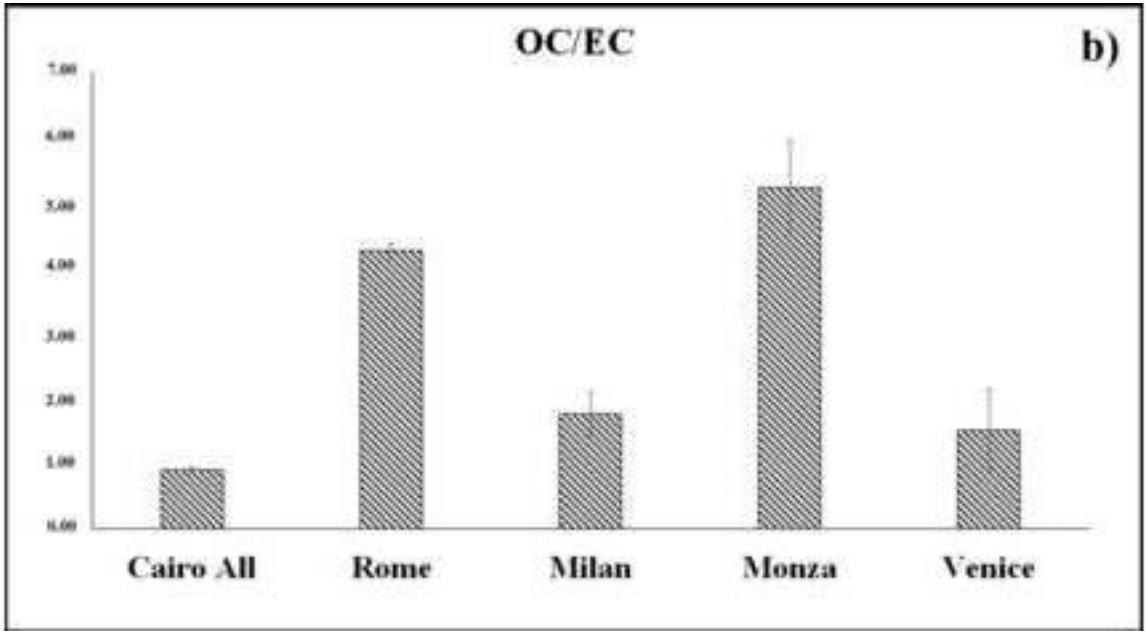

Supplementary material for on-line publication only

Click here to download Supplementary material for on-line publication only: Supplementary material.pptx

***conflict of Interest Statement**

Declaration of interests

☒ The authors declare that they have no known competing financial interests or personal relationships that could have appeared to influence the work reported in this paper.

☐The authors declare the following financial interests/personal relationships which may be considered as potential competing interests:

Author contributions

Natalia Rovella, **Writing - Original Draft, Writing - Review & Editing, Validation, Formal analysis, Investigation**

Nevin Aly, **Writing - Review & Editing, Investigation**

Valeria Comite, **Formal analysis, Writing - Original Draft, Investigation , Methodology**

Luciana Randazzo, **Formal analysis, Investigation, Data Curation, Methodology**

Paola Fermo, **Writing - Review & Editing, Data Curation**

Donatella Barca, **Formal analysis, Data Curation,**

Monica Alvarez de Buergo, **Writing - Review & Editing**

Mauro Francesco La Russa, **Supervision, Writing - Review & Editing, Funding acquisition, Project administration**